FAST INVERSE TONE MAPPING WITH REINHARD'S GLOBAL OPERATOR

Yuma Kinoshita, Sayaka Shiota and Hitoshi Kiya

Tokyo Metropolitan University
Department of Information and Communication Systems
Tokyo, Japan

ABSTRACT

This paper proposes a novel inverse TMO, which enables to generate HDR images from LDR ones, not only without using any specific parameters but also at low computing costs. Furthermore, the inverse TMO has a new characteristic when an LDR image is mapped from an HDR one by Reinhard's global operator. In the case, the HDR image reconstructed by the proposed method without parameters can be remapped into the same image as that remapped from an HDR one reconstructed with parameters. Experimental results show that the proposed inverse tone mapping (TM) operation can be carried out, while keeping better structural similarity and lower computing cost than conventional methods.

Index Terms— high dynamic range, inverse tone mapping, tone mapping, HDR imaging, image enhancement

1. INTRODUCTION

The interest of high dynamic range (HDR) imaging has recently been increasing in various area: photography, medical imaging, computer graphics, on vehicle cameras and astronautics. They have wider dynamic range of pixel values than standard low dynamic range (LDR) images. To visualize HDR images and videos, HDR displays have been developed. The most common approach to produce HDR images with a LDR detector is to sequentially capture multiple images of the same scene using different exposures [1, 2]. However, this kind of approaches is only suitable for static scenes. In addition, these approaches are not suitable for reproducing real-world appearance images through legacy LDR images or videos. Therefore, a number of inverse tone mapping operators (TMOs) for dynamic range expansion have been proposed to visualize LDR images on HDR devices.

Various research works on inverse TM have so far been done [3–7]. Huo et al. succeeded in expanding the local dynamic range in dark and bright area by using the dodging and burning algorithm with a S curve operator [6]. Wang et al. proposed an inverse TM operation which conflates pseudo-multiple-exposures HDR images generated from a

single LDR image [7]. In addition, the inverse TM is used not only to generate an HDR image from an LDR one, but also to compression coding an HDR image such as JPEG-XT standard [8]. A high-performance inverse TM operation at low computational costs is required because HDR imaging techniques are expected to apply to not only images but also videos. However, the existing inverse TM operations require a lot of calculation for generating high quality HDR images. For example, the Banterle et al.'s method [3] has complex processing such as bilateral filtering and the median cut algorithm. This is due to a loss of information about the dynamic range of the real scene.

To overcome these problems, we propose a novel inverse TMO based on the existing TMO. Many research works on TM operations which generate an LDR image from an HDR image have been studing [9–16]. The proposed inverse TMO, which is based on a inverse transform of Reinhard's global operator [17,18], allows to be carried out not only without any parameters but also without any data-depended calculation.

Furthermore, the proposed one has another application i.e. remapping LDR images into other LDR ones with desirable quality. When an LDR image is mapped from an HDR one by Reinhard's global operator [17], the HDR images reconstructed by the proposed method can be remapped into the same image as that remapped from an HDR one reconstructed with parameters. Therefore, the proposed inverse TMO also allows to efficiently store HDR images as LDR ones by conventional image coding methods such as JPEG, JPEG2000 and HEVC.

We evaluate the effectiveness of the proposed inverse TMO in terms of the quality of generated HDR images and the executing time by a number of simulations. Simulation results show that the proposed method is able to remap LDR ones mapped by Reinhard's global TMO, with high quality. In addition, it is confirmed that the proposed method is to effectively perform inverse TM maintaining the structural similarity with a low computational cost.

2. PREPARATION

A TM operation generates an LDR image I_L from an HDR image I_H. A typical TM operation is reviewed.

2.1. Photographic Tone Reproduction

"Photographic Tone Reproduction" [17] which is a typical TM operation is summarized, here. This TM operation consists of the following six steps.

(a) The world luminance $L_w(p)$ of an HDR image I_H is calculated from RGB pixel values of the HDR one as,

$$L_w(p) = 0.27R(p) + 0.67G(p) + 0.06B(p) \quad (1)$$

where $R(p)$, $G(p)$ and $B(p)$ are RGB pixel values of the HDR image with a pixel p, respectively.

(b) The geometric mean $\overline{L}_w$ of the world luminance $L_w(p)$ is calculated as follows:

$$\overline{L}_w = \exp\left(\frac{1}{N}\sum_{p=1}^{N}\log L_w(p)\right) \quad (2)$$

where N is the total number of pixels in the input HDR image I_H.

(c) The scaled luminance $L(p)$ is calculated as

$$L(p) = \frac{\alpha}{\overline{L}_w}L_w(p) \quad (3)$$

where $\alpha \in [0,1]$ is the parameter called "key value", which indicates subjectively if the scene is light, normal, or dark [17]. α corresponds to the geometric mean of the scaled luminance.

(d) The display luminance $L_d(p)$ is calculated by using a TMO $y(\cdot)$ as follows:

$$L_d(p) = y(L(p)). \quad (4)$$

The Reinhard's global operator [17] which is a well-known TMO is given by

$$L_d(p) = \frac{L(p)}{1 + L(p)}. \quad (5)$$

(e) The floating-point pixel values $C_f(p)$ of the LDR image is calculated as follows:

$$C_f(p) = \frac{L_d(p)}{L_w(p)}C(p) \quad (6)$$

where $C(p) \in \{R(p), G(p), B(p)\}$ is the floating-point RGB value of the input HDR image I_H, and $C_f(p) \in \{R_f(p), G_f(p), B_f(p)\}$. Besides, the gamma correction is performed for $C_f(p)$ as needed.

(f) The 8-bit color RGB values $C_i(p)$ of the LDR image I_{Lg} is derived from

$$C_i(p) = \text{round}(C_f(p) \cdot 255) \quad (7)$$

where round(x) rounds x to its nearest integer value, and $C_i(p) \in \{R_i(p), G_i(p), B_i(p)\}$.

2.2. Scenarios

This paper proposes a novel inverse TMO to estimate HDR images from LDR ones. We have two scenarios from the difference of applications.

Scenario 1: Inverse TM of existing LDR images

The first scenario is to estimate HDR images from existing LDR ones captured in legacy LDR format as shown in Fig. 1. In this case, there is no information on the relation-
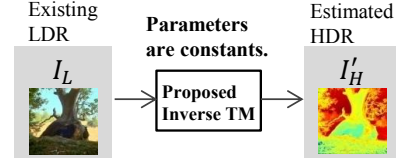
Fig. 1. 1st scenario
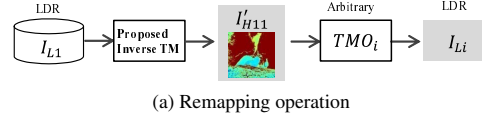
(a) Remapping operation
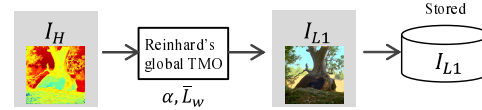
(b) 1st TM

Fig. 2. 2nd scenario

ship between the LDR ones and the real scenes. Therefore, it is difficult to determine operators or parameters for inverse TM. As a result, conventional inverse TM operations require high computing cost processing for generating high quality HDR images from existing LDR ones.

By using the proposed method, fast inverse TM is able to carry out without any parameters even when LDR images are not generated by Reinhard's global operator.

Scenario 2: remapping LDR images

The second scenario is to remap LDR images to other LDR ones with different qualities by using arbitrary TMO shown in Fig. 2(a). In the scenario, the first TMO is the Reinhard's global operator (see Fig. 2(b)). The second is an arbitrary TMO such as a local TMO, which can provide an LDR image with desirable quality. Before the second TMO, an inverse TM operation is required. Conventionally, two parameters i.e. α and $\overline{L}_w$ have to be stored to conduct it. In contrast, the proposed inverse TM operation do not require the use of the parameters. In the case, the proposed inverse TMO has a new characteristic that an HDR image reconstructed by the proposed method without parameters can be remapped into the same image I_{Li} as that remapped from an HDR one reconstructed with parameters.

3. PROPOSED INVERSE TM OPERATION

Assuming the use of the Reinhard's global operator, a new inverse TM operation based on photographic tone reproduction is proposed.

3.1. Inverse TMO based on the Reinhard's TMO

The inverse function of the Reinhard's global operator is given as, from eqs.(3) and (5).

$$L_w(p) = \frac{\overline{L}_w}{\alpha} \cdot L(p) = \frac{\overline{L}_w \cdot L_d(p)}{\alpha(1 - L_d(p))} \quad (8)$$

where
$$L(p) = \frac{L_d(p)}{1 - L_d(p)}. \qquad (9)$$

It is confirmed that the key value α and the geometric mean $\overline{L}_w$ are necessary to calculate eq.(8). Therefore, these parameters or original HDR images are required to be stored.

By contrast, the proposed inverse TMO which does not use the parameters is shown below.
$$L'_w(p) = \frac{G}{A} \cdot L(p) = \frac{G \cdot L_d(p)}{A(1 - L_d(p))} \qquad (10)$$

where A, G is constant values. The above equation corresponds to the function substituted by $\alpha = A$ and $\overline{L}_w = G$ in eq.(8) respectively.

3.2. Proposed procedure

The procedure for Scenario 1 is summarized as follows.

1. Calculate a display luminance $L_d(p)$ from RGB values of an LDR image as
$$L_d(p) = \frac{0.27R_i(p) + 0.67G_i(p) + 0.06B_i(p)}{255}. \qquad (11)$$

2. Calculate a world luminance $L'_w(p)$ by eqs. (11) and (10).

3. Obtain an HDR image I'_H with color components $C'(p) \in \{R'(p), G'(p), B'(p)\}$ as follows:
$$C'(p) = \frac{L'_w(p)}{L_d(p)} \cdot C_f(p) = \frac{L'_w(p)}{L_d(p)} \cdot \frac{C_i(p)}{255}. \qquad (12)$$

3.3. Deriving the proposed inverse TMO

We discuss the validity that the parameters can be arbitrary values in the proposed inverse TMO.

First, we consider remapping an inverse mapped image by eq. (10) based on Photographic tone reproduction. The geometric mean $\overline{L}'_w$ of an inverse mapped image is calculated by substituting eq. (10) into eq. (2),
$$\overline{L}'_w = \exp\left(\frac{1}{N}\sum_{p=1}^{N}\log\frac{G \cdot L_d(p)}{A(1 - L_d(p))}\right)$$
$$= \frac{G}{A}\exp\left(\frac{1}{N}\sum_{p=1}^{N}\log L(p)\right) = \frac{G}{A} \cdot \alpha. \qquad (13)$$

Then, the scaled luminance $L'(p)$ for the second TMO is represented as, from eqs. (3) and (10)
$$L'(p) = \frac{\alpha'}{\overline{L}'_w} \cdot L'_w(p) = \frac{\alpha'}{\overline{L}'_w} \cdot \frac{G \cdot L_d(p)}{A(1 - L_d(p))}. \qquad (14)$$

By substituting eq. (13) into eq. (14),
$$L'(p) = \frac{\alpha'}{\alpha} \cdot \frac{L_d(p)}{1 - L_d(p)} \qquad (15)$$

where α' is a key value for the second TMO. From eq. (15), the display luminance $L'_d(p)$ of the remapped image is provided by
$$L'_d(p) = y(L'(p)) = y\left(\frac{\alpha'}{\alpha} \cdot \frac{L_d(p)}{1 - L_d(p)}\right). \qquad (16)$$

Note that there are no constants A and G.

On the other hand, if α and $\overline{L}_w$ are known, the geometric

mean $\overline{L}''_w$ of the inverse mapped image is calculated from eq. (8)
$$\overline{L}''_w = \exp\left(\frac{1}{N}\sum_{p=1}^{N}\log\frac{\overline{L}_w \cdot L_d(p)}{\alpha(1 - L_d(p))}\right) = \overline{L}_w. \qquad (17)$$

Then, the scaled luminance $L''(p)$ for the second TMO is represented as, in a similar way to $L'(p)$.
$$L''(p) = \frac{\alpha'}{\overline{L}''_w} \cdot L''_w(p) = \frac{\alpha'}{\overline{L}''_w} \cdot \frac{\overline{L}_w \cdot L_d(p)}{\alpha(1 - L_d(p))}$$
$$= \frac{\alpha'}{\alpha} \cdot \frac{L_d(p)}{1 - L_d(p)} \qquad (18)$$

Therefore, the display luminance $L''_d(p)$ of the remapped image is provided by
$$L''_d(p) = y(L''(p)) = y\left(\frac{\alpha'}{\alpha} \cdot \frac{L_d(p)}{1 - L_d(p)}\right). \qquad (19)$$

By comparing eq. (16) with eq. (19), we arrive at the relation:
$$L'_d(p) = L''_d(p). \qquad (20)$$

Hence, the remapped result by the proposed framework are the same image as the remapped one with the true parameters α and $\overline{L}_w$ regardless of the constants A and G. In this paper, $A = G = 1$ is used in the inverse TM for simplicity.

3.4. Evaluating the proposed method

HDR images generally have a much wider dynamic range than that of LDR ones. For this reason, conventional quality assessments such as PSNR or SSIM are not suited to evaluate the quality of HDR images. Therefore, various research works on evaluating HDR images have so far been done [19]. In this paper, we use typical quality metrics i.e. HDR-VDP-2.2 [20] and PU encoding [21] + MS-SSIM [22] to evaluate the quality of HDR images.

To evaluate the quality of HDR images, reference HDR images are needed. Generally, there are no reference HDR ones in LDR datasets. Thereby, we choose HDR images from HDR image dataset and generates LDR ones from these HDR ones by various TMOs.

4. SIMULATION

We evaluate the proposed inverse TMO in terms of the quality of a generated HDR image I'_{H1} and the executing time by a number of simulations with HDR images.

4.1. Simulation conditions

We used 60 HDR images selected from the databases [23, 24] for the evaluation (see Fig. 3). The following procedure was carried out to evaluate the effectiveness.

1. Map an HDR image I_H to an LDR image I_{Li} by several TMOs TMO_i. In this simulation, we used 10 TMOs selected from the literature [25]

2. Carry out some inverse TMOs, referred to as $iTMO_j$ for I_{Li}, to obtain I'_{Hij}.

3. Evaluate the similarity between images I'_{Hij} and I_H, in accordance with the criterions i.e. HDR-VDP-2.2 MOS value [20] and PU encoding [21]+ MS-SSIM

adjuster   tree   memorial

Fig. 3. Examples of LDR images I_{Li} mapped by several TMOs

[22]. These are typical HDR image quality assessments for evaluating HDR images [19].

Five inverse TMOs, i.e. the proposed method, the conventional inverse operation using eq.(8) with the true parameters (α and $\overline{L}_w$), PMET [7], Kuo's method [5] and Huo's method [6], are compared. The proposed method and the conventional inverse operation are called inverse photographic tone reproduction (IPTR) in the following section. The simulation was run on a PC, with a 3.4GHz processor, a main memory of 16Gbytes and MATLAB R2014b.

4.2. Simulation results

Figure 4 illustrates the average executing time when each inverse TMOs are carried out 100 times for 60 images. From the figure, the proposed inverse TMO has much lower computational cost than the others. On the other hand, PMET has large computational cost.

Tables 1 and 2 denote the average values of similarities between HDR images were evaluated by HDR-VDP-2.2 $\in [0, 100]$ and PU encoding + MS-SSIM $\in [0, 1]$, whose lager score indicates a higher similarity between two images.

Table 1 shows that IPTR is able to inverse tone map LDR images mapped by Reinhard's global TMO with the highest quality. The proposed inverse TMO also has the corresponding property and is able to map LDR ones with higher quality than the others. By contrast, PMET has the best HDR-VDP-2.2 score which is the average of whole images.

Besides, IPTR with parameters provides better MS-SSIM score averagely as shown in table 2. The proposed inverse TMO provides better HDR images by comparing with the others whereas it is slightly inferior than IPTR with parameters Therefore, the proposed inverse TMO is effective to perform inverse TM maintaining the structural similarity compared with other inverse TMOs.

5. CONCLUSION

This paper has proposed a novel inverse TMO based on Reinhard's global operator. The proposed inverse TMO enables to generate HDR images from LDR ones, not only without using any specific parameters but also at low computing costs. Furthermore, the inverse TMO has a characteristic when an LDR image is mapped by Reinhard's global operator. That is, an HDR image reconstructed by the proposed
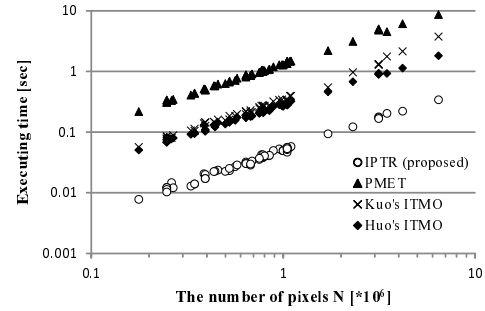
Fig. 4. Executing time of inverse TMOs

Table 1. Experimental results (HDR-VDP-2.2)

inverse TMO	IPTR (proposed)	IPTR (with parameters)	PMET	Kuo's ITMO	Huo's ITMO
Reinhard's global	56.13	61.85	53.38	43.48	52.76
Reinhard's local	37.48	38.52	44.69	42.04	42.90
Gamma TMO	34.88	35.95	41.27	40.33	38.54
Chiu's TMO	39.48	40.02	45.17	44.79	44.10
Fattal's TMO	41.42	41.34	44.41	44.71	45.76
Average (10 TMOs)	42.99	43.11	46.53	43.33	45.48

Table 2. Experimental results (PU encoding + MS-SSIM)

inverse TMO	IPTR (proposed)	IPTR (with parameters)	PMET	Kuo's ITMO	Huo's ITMO
Reinhard's global	0.918	0.976	0.860	0.597	0.831
Reinhard's local	0.866	0.917	0.860	0.596	0.818
Gamma TMO	0.772	0.752	0.833	0.514	0.754
Chiu's TMO	0.840	0.857	0.785	0.667	0.777
Fattal's TMO	0.840	0.815	0.741	0.672	0.787
Average (10 TMOs)	0.843	0.856	0.804	0.611	0.797

method without parameters can be remapped into the same image as that remapped form an HDR one reconstructed with parameters. The simulation results showed that the proposed inverse TMO is able to perform inverse TM maintaining better structural similarity at lower computing costs than other inverse TMOs.

6. REFERENCES

[1] P. E. Debevec and J. Malik, "Recovering high dynamic range radiance maps from photographs," in *ACM SIGGRAPH 2008 classes.* ACM, 2008, p. 31.

[2] S. K. Nayar and T. Mitsunaga, "High dynamic range imaging: Spatially varying pixel exposures," in *Computer Vision and Pattern Recognition, 2000. Proceedings. IEEE Conference on*, vol. 1. IEEE, 2000, pp. 472–479.

[3] F. Banterle, P. Ledda, K. Debattista, and A. Chalmers,

"Inverse tone mapping," in *Proceedings of the 4th international conference on Computer graphics and interactive techniques in Australasia and Southeast Asia*. ACM, 2006, pp. 349–356.

[4] A. G. Rempel, M. Trentacoste, H. Seetzen, H. D. Young, W. Heidrich, L. Whitehead, and G. Ward, "Ldr2hdr: on-the-fly reverse tone mapping of legacy video and photographs," *ACM Transactions on Graphics (TOG)*, vol. 26, no. 3, p. 39, 2007.

[5] P.-H. Kuo, C.-S. Tang, and S.-Y. Chien, "Content-adaptive inverse tone mapping," in *Visual Communications and Image Processing (VCIP)*. IEEE, 2012, pp. 1–6.

[6] H. Youngquing, Y. Fan, and V. Brost, "Dodging and burning inspired inverse tone mapping algorithm," *Journal of Computational Information Systems*, vol. 9, no. 9, pp. 3461–3468, 2013.

[7] T.-H. Wang, C.-W. Chiu, W.-C. Wu, J.-W. Wang, C.-Y. Lin, C.-T. Chiu, and J.-J. Liou, "Pseudo-multiple-exposure-based tone fusion with local region adjustment," *Multimedia, IEEE Transactions on*, vol. 17, no. 4, pp. 470–484, 2015.

[8] ISO/IEC, "ISO/IEC 18477 Information technology - Scalable compression and coding of continuous-tone still images," 2015.

[9] N. Banić and S. Lončarić, "Puma: A high-quality retinex-based tonemapping operator," in *2016 24th European Signal Processing Conference (EUSIPCO)*, 2016, pp. 943–947.

[10] Z. Zhu, Z. Li, S. Wu, and P. Fränti, "Noise reduced high dynamic range tone mapping using information content weights," *Acoustics, Speech and Signal Processing (ICASSP), 2015 IEEE International Conference on*, pp. 1255–1259, 2015.

[11] J. Duan and G. Qiu, "Fast tone mapping for high dynamic range images," in *Pattern Recognition, 2004. ICPR 2004. Proceedings of the 17th International Conference on*, vol. 2. IEEE, 2004, pp. 847–850.

[12] S. Thakur, M. Sivasubramanian, K. Nallaperumal, K. Marappan, and N. Vishwanath, "Fast tone mapping for high dynamic range images," in *Computational Intelligence and Computing Research (ICCIC), 2013 IEEE International Conference on*. IEEE, 2013, pp. 1–4.

[13] T. Dobashi, A. Tashiro, M. Iwahashi, and H. Kiya, "A fixed-point implementation of tone mapping operation for hdr images expressed in floating-point format," *APSIPA Trans. Signal and Information Processing*, vol. 3, no. e11, pp. 1–11, 2014.

[14] T. Murofushi, M. Iwahashi, and H. Kiya, "An integer tone mapping operation for hdr images expressed in floating point data," in *2013 IEEE International Conference on Acoustics, Speech and Signal Processing*. IEEE, 2013, pp. 2479–2483.

[15] T. Murofushi, T. Dobashi, M. Iwahashi, and H. Kiya, "An integer tone mapping operation for hdr images in openexr with denormalized numbers," in *2014 IEEE International Conference on Image Processing (ICIP)*. IEEE, 2014, pp. 4497–4501.

[16] T. Dobashi, T. Murofushi, M. Iwahashi, and H. Kiya, "A fixed-point tone mapping operation for hdr images in the rgbe format," in *Proc. APSIPA Annual Summit and Conference*. APSIPA, 2013, pp. 1–4.

[17] E. Reinhard, M. Stark, P. Shirley, and J. Ferwerda, "Photographic tone reproduction for digital images," *ACM Transactions on Graphics (TOG)*, vol. 21, no. 3, pp. 267–276, 2002.

[18] E. Reinhard, W. Heidrich, P. Debevec, S. Pattanaik, G. Ward, and K. Myszkowski, *High dynamic range imaging: acquisition, display, and image-based lighting*. Morgan Kaufmann, 2010.

[19] P. Hanhart, M. V. Bernardo, M. Pereira, A. M. Pinheiro, and T. Ebrahimi, "Benchmarking of objective quality metrics for hdr image quality assessment," *EURASIP Journal on Image and Video Processing*, vol. 2015, no. 39, 2015.

[20] M. Narwaria, R. K. Mantiuk, M. P. Da Silva, and P. Le Callet, "Hdr-vdp-2.2: a calibrated method for objective quality prediction of high-dynamic range and standard images," *Journal of Electronic Imaging*, vol. 24, no. 1, 2015.

[21] T. O. Aydın, R. Mantiuk, and H.-P. Seidel, "Extending quality metrics to full dynamic range images," in *Human Vision and Electronic Imaging XIII*, ser. Proceedings of SPIE, San Jose, USA, January 2008, pp. 6806–10.

[22] Z. Wang, E. P. Simoncelli, and A. C. Bovik, "Multi-scale structural similarity for image quality assessment," in *Signals, Systems and Computers, 2004. Conference Record of the Thirty-Seventh Asilomar Conference on*, vol. 2. IEEE, 2003, pp. 1398–1402.

[23] "Github - openexr." [Online]. Available: https://github.com/openexr/

[24] "High dynamic range image examples." [Online]. Available: http://www.anyhere.com/gward/hdrenc/pages/originals.html

[25] F. Banterle, A. Artusi, K. Debattista, and A. Chalmers, *Advanced High Dynamic Range Imaging: Theory and Practice*. Natick, MA, USA: AK Peters (CRC Press), 2011.